Sustainable Food Technology

ROYAL SOCIETY OF CHEMISTRY

PAPER

View Article Online
View Journal



Cite this: DOI: 10.1039/d5fb00583c

# Harnessing machine learning for chicken meat quality evaluation using curcumin-loaded methylcellulose intelligent films

Suresh Chandra Varsha,†[ab] Ashique Thazheparamban†[ab] and Arunkumar Panneerselvam *[ab]

Received 10th September 2025
Accepted 24th March 2026

DOI: 10.1039/d5fb00583c

rsc.li/susfoodtech

In this study, curcumin (Cur) was incorporated into a methylcellulose (MC) biopolymer to develop an intelligent packaging system for real-time monitoring of chicken meat freshness (at 4 ± 2 °C), using machine learning (ML). Artificial neural network (ANN)-based classification and regression models were developed to predict the freshness of chicken meat by analysing colourimetric changes in the MC/3.0% Cur intelligent film. The models were trained using the colour response of the intelligent film to various concentrations (0–1200 ppm) of biogenic amines (histamine, tyramine, putrescine, cadaverine, or spermine). Colour features were quantitatively extracted from digital images of the intelligent film in RGB (Red, Green, Blue), CIE *Lab** (lightness, green-red, blue-yellow), and HSV (Hue, Saturation, Value) colour spaces. The ANN regression model achieved a high $R^2$ of 0.928, with a low root mean square error (RMSE) of 1.99 (mg N/100 g) for total volatile basic nitrogen (TVB-N) prediction in test-set data, demonstrating precise quantification. The ANN classification model demonstrated 96.5% accuracy in categorising test-set data into fresh, semi-fresh, or spoiled states. The models were applied to predict chicken meat freshness; the classification model accurately predicted freshness, while the regression model showed an $R^2$ of 0.901 between predicted and experimental TVB-N values.

**Sustainability spotlight**

This study demonstrates that curcumin-loaded methylcellulose intelligent films, combined with machine learning (ML) models, can provide real-time monitoring of chicken meat spoilage through smartphone-based analysis, thereby aligning with United Nations Sustainable Development Goal (SDG) 3 (Good Health and Well-being). The use of biodegradable, plant-derived raw materials reduces dependence on petroleum-based plastics and helps curb food waste through freshness detection, directly contributing to SDG 12 (Responsible Consumption and Production). Furthermore, integrating ML with a web-based application aligns with SDG 9 (Industry, Innovation and Infrastructure), demonstrating that digital innovation can be harnessed to develop scalable, sustainable food technologies.

## 1 Introduction

Chicken is a globally consumed meat, yet its highly perishable nature and susceptibility to pathogen growth, such as *Salmonella* and *Campylobacter*, pose significant food safety challenges, often stemming from improper handling and storage.[1,2] Contamination can occur at various stages, from slaughter to retail, necessitating robust monitoring strategies.[1,2] Given the substantial public health risks associated with consuming spoiled chicken meat, real-time assessment of its freshness is vital.

The microbial spoilage of chicken meat is accompanied by the production of volatile compounds such as ammonia, biogenic amines, and $CO_2$, which can serve as freshness indicators.[3] Among the critical indicators of chicken meat quality, the release of biogenic amines during spoilage has gained attention owing to its association with microbial and enzymatic activity.[4] Biogenic amines are nitrogenous compounds primarily produced by microbial decarboxylation of amino acids, including lysine (cadaverine), arginine (putrescine), histidine (histamine), and tyrosine (tyramine), while polyamines such as spermidine and spermine are formed from putrescine.[5] These compounds contribute to the off-flavours and odours associated with meat spoilage, thereby serving as an indirect marker of microbial degradation. The concentration of biogenic amines is often measured as total volatile basic nitrogen (TVB-N), a widely recognised parameter for evaluating meat spoilage.[6] TVB-N production leads to an inherent increase in the pH of chicken meat. The pH-sensitive intelligent films incorporating halochromic indicators such as curcumin,[6]

[a]Department of Food Packaging Technology, CSIR-Central Food Technological Research Institute, Mysuru, 570020, India. E-mail: arunpselvam.cftri@csir.res.in
[b]Academy of Scientific and Innovative Research (AcSIR), Ghaziabad, 201002, India
† These authors contributed equally.

anthocyanins,[7] betalains,[8] alizarin,[9] and shikonin[10] have been extensively explored for monitoring meat freshness, particularly by detecting biogenic amines in the headspace of packaged meat products.

Curcumin (Cur), a natural polyphenol derived from turmeric, is a promising halochromic indicator due to its distinct pH-sensitive colour changes. In neutral conditions, it appears yellow due to its keto form. As the pH becomes alkaline, the colour changes to reddish brown, driven by keto-enol tautomerisation.[11] This distinct colour-changing property of curcumin can be used to detect biogenic amines. Cur has been integrated into biopolymer matrices such as chitosan/polyethene oxide,[6] κ-carrageenan,[12] gelatin,[13] and polylactic acid[14] to develop intelligent food packaging systems. However, these matrices contain ionisable functional groups that can buffer pH changes, potentially limiting colourimetric sensitivity. In contrast, this study utilises methylcellulose (MC), a non-ionic cellulose ether with high optical clarity and minimal intrinsic pH-buffering capacity.[15] This allows for distinct and rapid colourimetric responses to spoilage-related volatiles, improving sensitivity. Furthermore, MC, Cur, and glycerol are food additives that offer a sustainable, cost-effective, and scalable option for commercial adoption.

Traditionally, assessing food freshness using intelligent packaging has predominantly relied on visual observation, *i.e.*, colour changes in the intelligent films. This approach is susceptible to human error and possesses limited sensitivity to subtle variations in spoilage indicators. However, integrating machine learning (ML) models enables consumers to capture images of the intelligent film *via* smartphones and use a trained model to analyse colour shifts and predict the meat freshness.[16,17] For the development of the ML model, various colour spaces such as RGB (Red, Green, Blue), CIE (Commission Internationale de l'Eclairage) $L^*a^*b^*$ (lightness, green-red, blue-yellow), and HSV (Hue, Saturation, Value), are widely used for feature extraction.[17,18]

RGB colour space captures the fundamental colour composition by measuring the intensity of red, green, and blue light. In contrast, HSV colour space separates the value (brightness) from the colour components, hue and saturation. Hue, which directly relates to the perceived colour (such as red, blue, or yellow), is often more intuitive than raw RGB values for identifying colour changes associated with spoilage. Saturation captures the colour's purity, providing additional information about its vibrancy. This makes HSV useful for distinguishing colours under different lighting conditions.[18] On the other hand, the $L^*a^*b^*$ colour space is designed to align more closely with human perception of colour differences. $L^*$ represents lightness, allowing for the analysis of brightness independently of chromaticity, while $a^*$ and $b^*$ values represent the colour axes (red to green and yellow to blue, respectively), providing a precise measure of colour shifts.[18]

The aim of the study is to develop and validate classification and regression models using colourimetric data extracted from MC/3.0% Cur intelligent film. The classification models using logistic regression, support vector classifier (SVC), decision trees, and artificial neural network (ANN) categorise chicken meat into fresh, semi-fresh, or spoiled states, critical for consumer safety. Conversely, regression models [linear regression, ANN, and support vector regression (SVR)] predict specific TVB-N concentrations, providing quantitative data valuable for supply chain quality control. These ML model algorithms, although basic, are widely used and provide reliable methodologies for meat spoilage detection and quality assessment. The performance of these models was validated against experimentally measured TVB-N values of chicken meat stored under refrigerated conditions ($4 \pm 2$ °C).

# 2 Materials and methods

## 2.1 Materials

Curcumin, DPPH (2,2-diphenyl-1-picrylhydrazyl), magnesium oxide, and methylcellulose were sourced from HiMedia Laboratories (P) Ltd, India. Biogenic amine standards (histamine, tyramine, putrescine, spermine), boric acid, hydrochloric acid, anhydrous calcium chloride, and glycerol were obtained from Sisco Research Laboratories (P) Ltd, India. Ethanol and cadaverine were procured from Sigma Aldrich. ABTS [2,2′-azino-bis(3-ethylbenzothiazoline-6-sulfonic acid)] and potassium persulfate were purchased from Central Drug House (P) Ltd, India. High-purity deionised water was obtained from the Millipore Milli-Q system.

## 2.2 Preparation of MC and MC/Cur films

MC and MC/Cur films were prepared by solution casting. 3 g of MC was dissolved in 100 mL of deionised water, and 300 μL of glycerol was added as a plasticiser. Different concentrations of Cur (0.5, 1.0, or 3.0 wt% of MC) dissolved in ethanol were added to the above solution, which was further stirred for 3 hours, then carefully cast onto polytetrafluoroethylene film-pasted glass plates and dried under infrared (IR) light. MC films were prepared using the same technique without the addition of Cur. After drying, the films were carefully peeled off and stored at $25 \pm 1$ °C and $65 \pm 2$% relative humidity (RH) for 48 h prior to analysis.

## 2.3 Characterisation of films

**2.3.1 Structural, morphological, and moisture barrier properties.** The neat MC and MC/Cur films were analysed by attenuated total reflectance-Fourier transform infrared (ATR-FTIR) (Bruker ATR-FTIR spectrometer, Tensor II, Germany, 400–4000 $cm^{-1}$ wavenumber range at a 4 $cm^{-1}$ resolution in transmittance mode) to identify the functional groups and by scanning electron microscopy (SEM, Zeiss, Germany) to analyse the surface morphology. The films were sputtered with gold prior to SEM analysis. To assess thickness, film samples (10 cm × 2 cm) were measured using a digital micrometre (0.01 mm, MI20 TMI Messmer Instruments, UK), with six measurements taken at random points per sample; the mean was used. The water contact angles of the neat MC and MC/Cur films were determined in triplicate to evaluate their hydrophobicity, using a sessile drop contact angle goniometer (Kruss DSA 30 E, Germany). A deionised water (8 μL) droplet was gently placed onto the film surface, and the contact angle was measured after 5 seconds at $24 \pm 1$ °C. The water vapour permeability (WVP) of the developed films was determined using the desiccant

 

method according to ASTM E 96/96M-24.[19] Calcium chloride was used as a desiccant and placed inside aluminium cups sealed with the developed films. The cups were then kept in a humidity chamber at 38 ± 1 °C and 90 ± 1% RH. The weight gain of the cup over time was determined using the following formula: triplicate measurements are reported.

$$\mathrm{WVP} = \frac{b \times L}{A \times P}$$

where $b$ is the slope of the weight change of the cup over time (g $s^{-1}$), $L$ is the thickness of the film (m), $P$ is the water vapour pressure difference (Pa) across the film, and $A$ is the surface area of the film ($m^2$).

**2.3.2 Mechanical properties.** Tensile strength ($T_s$), Young's modulus ($Y_m$), and % elongation at break (%E) of MC and MC/(0.5–3.0%) Cur films were measured as averages of six replicates using a LLOYD Universal Testing Machine (LLOYD-LR-10 K, France, Europe) as per ASTM-D882-18 standard.[20] Rectangular strips (10 cm × 2 cm) were cut from the films, and tests were performed with a 50 mm gauge length and a crosshead speed of 50 mm $min^{-1}$.

**2.3.3 Antioxidant and UV blocking properties.** The antioxidant activity of MC and MC/Cur films was measured in triplicate using the DPPH free radical scavenging assay. Film samples (50 mg) were immersed in 10 mL of 0.1 mM DPPH ethanolic solution, shaken vigorously, and incubated in the dark for 30 minutes. After incubation, the reduction in absorbance of the unfiltered clear solution was measured at 517 nm using a UV-Vis spectrophotometer (Hitachi U-5300). The antioxidant property of MC and MC/Cur films was calculated using the following formula:[21]

$$\text{DPPH free radical scavenging activity}(\%) = \frac{A_c - A_s}{A_c} \times 100$$

where $A_c$ = absorbance of DPPH and $A_s$ = absorbance of film samples.

For the ABTS assay, ABTS radical stock solution was prepared by mixing 7 mM ABTS and 2.45 mM potassium persulfate, incubating in the dark for 16 hours, and diluting to an absorbance of 0.70 ± 0.03 at 734 nm. Film samples (50 mg in 10 mL deionised water) were mixed with the diluted ABTS solution (100 μL sample + 900 μL ABTS), and the absorbance of the clear unfiltered solution was recorded at 734 nm. The ABTS scavenging activity was calculated using the following formula[21] and reported as an average of three replicates.

$$\text{ABTS scavenging effect}(\%) = \frac{A_c - A_s}{A_c} \times 100$$

Here, $A_c$ = absorbance of ABTS, $A_s$ = absorbance of the film samples.

The UV blocking (280–400 nm) and transmittance in the visible region of the MC or MC/Cur films were recorded in triplicate using a double-beam UV-Vis spectrophotometer (Hitachi, UH5300). The % UV blocking for the films was calculated using the formula:

$$\%\ \text{UV blocking} = 100 - \%\ \text{transmittance}$$

### 2.4 Design of experiment

To evaluate the dose-dependent response of the MC/3.0% Cur intelligent film to biogenic amines produced during chicken meat spoilage, various concentrations (0, 1, 10, 50, 100, 200, 300, 400, 500, 600, 900, and 1200 ppm) of cadaverine, putrescine, histamine, spermine, and tyramine were prepared and sealed in 5 mL glass vials. The intelligent film (1 cm × 1 cm) was affixed to the vial's cap, and the film's colour changes were assessed by capturing digital photos after 2 hours incubation period. These images were subsequently used to train the ML models.

**2.4.1 Data collection, processing, and feature selection.** Digital images of the biogenic amine-exposed films were captured using a Samsung Galaxy S21 FE smartphone under consistent, controlled lighting conditions to minimise external variability. The dataset consists of 944 images, representing 60 distinct experimental conditions (5 biogenic amines at 12 different concentrations). To manage the input dimensionality for the ML model, the raw images were not used directly; instead, the average RGB value of the image was extracted using the skimage Python library to represent the image for further analysis. These were subsequently transformed into HSV and *Lab** colour spaces to provide a comprehensive representation of various colours. By reducing the input from pixel arrays to a 9-element feature vector, the sample-to-feature ratio was increased. This reduction in dimensionality is intended to mitigate overfitting and allow the ML model to converge on the specific colourimetric shifts associated with TVB-N concentration.

During data processing, $L^*$ and value were excluded from the feature set because they primarily reflect brightness, making them less relevant for detecting colour changes caused by biogenic amines in the MC/3.0% Cur intelligent film. Additionally, all remaining features were transformed using the natural logarithmic scale, resulting in 14 features [Red, Green, Blue, $a^*$ *Lab*, $b^*$ *Lab*, Hue, Saturation, Log-Green, Log-Red, Log-Blue, Log-$a^*$ *Lab*, Log-$b^*$ *Lab*, Log-Hue, Log-Saturation].

Furthermore, the biogenic amine concentrations were converted from ppm to mg N/100 g for subsequent ML model training. For the classification model, the extracted data were labelled as fresh (film exposed to <10 mg N/100 g; 707 instances), semi-fresh (film exposed to 10 to <20 mg N/100 g; 157 instances), or spoiled (film exposed to ≥20 mg N/100 g; 80 instances). Furthermore, to address imbalanced class distributions in the dataset, minority class over-sampling was employed before training the classification model. As feature selection is crucial for optimal ML model training, $b^*$ *Lab* (yellowness of the film), log-hue (representing overall colour of the image), and saturation were chosen from the data set for further analysis based on their strong correlation with TVB-N content (mg N/100 g) and relatively low correlations among each other (Fig. S1). To evaluate MC/3%Cur intelligent film sensitivity to biogenic amine concentrations, the colour difference ($\Delta E$) between unexposed and TVB-N-exposed films was calculated in the CIE Lab* colour space using the following formula.

$$\Delta E = \sqrt{(L1^* - L2^*)^2 + (a1^* - a2^*)^2 + (b1^* - b2^*)^2}$$

where $L1^*$, $a1^*$ and $b1^*$ are the CIE *Lab* colour values of the unexposed MC/3.0% Cur film. $L2^*$, $a2^*$ and $b2^*$ are the CIE *Lab* colour values of the TVB-N-exposed MC/3.0% Cur film.

**2.4.2 ML model training and evaluation.** In the pre-processing stage, the dataset was split 80:20 (training: testing) into subsets to ensure robust evaluation and avoid overfitting. Furthermore, the features were standardised using *Z*-score normalisation (which transforms the data to a standard normal distribution with a mean of 0 and a standard deviation of 1) to ensure that all features contributed equally to the model and to prevent features with larger magnitudes from dominating the learning process.[22] For each feature, the mean ($\mu$) and standard deviation ($\sigma$) were calculated. Then, each data point was transformed using the formula:

$$z = (x - \mu)/\sigma$$

where $z$ is the standardised value, and $x$ is the original value.

To develop models for predicting chicken meat freshness, linear regression, ANN, and SVR were employed for the regression model, while logistic regression, SVC, decision trees, and ANN were used for the classification model. The ANN model performed better in classification and regression models, hence it was selected for further analysis.

A grid search was conducted to optimise model parameters. For the classification model, two hidden layers with 50 neurons each used a 'relu' activation function, a maximum of 3000 iterations, and the 'adam' optimiser. Similarly, for the regression model, the optimal configuration included two hidden layers with 50 neurons each using a 'relu' activation function, with a regularisation parameter ($\alpha$) of 0.01, a constant learning rate, a maximum of 3000 iterations, and the 'adam' optimiser. All other model settings were maintained at their default values for both classification and regression models.

The performance of the ML models was evaluated using $R^2$, root mean square error (RMSE), accuracy, precision, recall, F1-score (harmonic mean of precision and recall), and the receiver operating characteristic area under the curve (ROC-AUC). A 10-fold stratified randomised cross-validation was employed to ensure robust and reliable results. All experiments were conducted using Python with the scikit-learn library.

$$\text{Accuracy} = \frac{\text{number of correct predictions}}{\text{total number of predictions}}$$

$$\text{Precision} = \frac{\text{true positives}}{\text{true positives} + \text{false positives}}$$

$$\text{Recall} = \frac{\text{true positives}}{\text{true positives} + \text{false negatives}}$$

$$\text{F1 score} = 2 \times \frac{(\text{precision} \times \text{recall})}{(\text{precision} + \text{recall})}$$

The ROC curve plots the true positive rate (recall) against the false positive rate (FPR) at various threshold settings, while the AUC-ROC provides a single value that summarises the overall performance.[17]

$$\text{FPR} = \frac{\text{false positives}}{\text{true negatives} + \text{false positives}}$$

AUC ranges from 0 to 1, with 1 indicating a perfect model and 0.5 indicating a model with no discriminative power.

### 2.5 Web-based application development

A web-based application was developed to enable real-time, user-friendly evaluation of chicken meat spoilage by integrating the trained classification model. The backend was developed in Python and deployed on a free cloud-hosted server (https://Render.com). The front-end was built using HTML, CSS, and JavaScript, and optimised for mobile devices to facilitate on-site assessment. Through the web application, users can sequentially capture the images of the unexposed and the chicken-meat-exposed MC/3.0% Cur intelligent film.

Upon successful capture of unexposed intelligent film, its colour values are compared to predefined standard colour values used during ML model training. If the deviation exceeds 15%, users are prompted to check lighting conditions or other possible errors. Following that, the users are prompted to capture the image of the chicken-meat-exposed intelligent film, and the colour data is transmitted to the backend server, where it is converted to the *Lab** colour space. The backend server computes a correction factor between the captured unexposed intelligent film colour and the predefined reference colour. This correction is applied to the exposed intelligent film in *Lab** space to compensate for illumination and camera-related colour shifts. The corrected *Lab** values are then converted to RGB and HSV colour spaces, followed by logarithmic transformation of selected features. The same scaler used during model training is applied for feature normalisation. These processed features are then input into the ML model, which returns the predicted stage of chicken meat freshness to the front end for user display.

### 2.6 Shelf-life evaluation of chicken meat

Skinless, boneless raw chicken meat was procured from a local butcher in Mysuru, India. The chicken meat samples (~3 g each) were cleaned and placed into 5 mL glass vials. The MC/3.0% Cur film was chosen for the study as it showed a good correlation between colour change and biogenic amine concentration. A 1 cm × 1 cm film was affixed to the vial cap, ~1 cm above the chicken meat samples, which were stored at 4 ± 2 °C (refrigerated condition). The colour changes in the intelligent film were captured using a Samsung Galaxy S21 FE smartphone (every 24 hours up to 120 hours). The experimental TVB-N and pH were analysed simultaneously at regular intervals (every 24 hours up to 120 hours). Then, the images are used to make predictions using the developed ML models.

**2.6.1 TVB-N and pH measurements.** The TVB-N content of the chicken meat samples was measured following the Chinese standard (GB 5009.228-2016) as described by Cai *et al.*[23] The chicken meat (~3 g) was homogenised with 50 mL of deionised water using an Ultra-Turrax T25 homogeniser (IKA, Germany) for 30 minutes. The resulting homogenate was filtered, and the filtrate was utilised for pH (Eutech pH 700, Singapore) and TVB-N analysis. Subsequently, 5 mL of the filtrate was distilled using a Kjeldahl distillation unit containing 5 mL of MgO suspension (10 g $L^{-1}$). The distillate was collected in a 10 mL boric acid solution (20 g $L^{-1}$) and titrated with 0.01 mol $L^{-1}$ HCl. The TVB-N content was then calculated and expressed in mg N/100 g.[12,23] All measurements were performed in triplicate.

$$\text{TVB-N}\left(\text{N}\frac{\text{mg}}{100\text{g}}\right) = \frac{(V_1 - V_2) \times 14 \times C}{m \times \frac{V_a}{V_t}} \times 100$$

$V_1$ = volume of HCl used for sample (mL); $V_2$ = volume of HCl used for blank (mL); $C$ = concentration of HCl (mol $L^{-1}$); $m$ = sample weight (g), $V_a$ = volume of filtrate distilled, and $V_t$ = total volume of the extract.

### 2.7 Statistical analysis

The experimental data on antioxidant, mechanical, UV-blocking, and moisture barrier properties were analysed using one-way analysis of variance (ANOVA) in SPSS version 12.0 (SPSS Inc., Chicago, IL, USA). Prior to ANOVA, the assumptions of normality and homogeneity of variance were verified using the Shapiro–Wilk test and Levene's test, respectively. Differences among means were evaluated using post hoc multiple comparison tests ($p < 0.05$). Results are expressed as mean ± standard deviation.

## 3 Results and discussion

### 3.1 ATR-FTIR spectroscopy

ATR-FTIR spectroscopy was used to evaluate molecular interactions between MC and varying concentrations of Cur (0.5%, 1.0%, or 3.0%) (Fig. S2). Neat MC films exhibited characteristic peaks at 3383 $cm^{-1}$ (–OH stretching), 2917 $cm^{-1}$ (C–H stretching of methoxy groups), and 1047 $cm^{-1}$ (C–O–C ether linkage), consistent with previous reports.[24,25] A new band at 1515 $cm^{-1}$, corresponding to C=C aromatic ring stretching, was observed in all Cur-loaded films, most distinctly for MC/3.0% Cur film, confirming Cur incorporation in the MC matrix.[26]

### 3.2 Surface morphology

SEM analysis revealed that the MC, 0.5% and 1.0% Cur reinforced MC films have smooth surfaces, indicating a uniform dispersion of Cur within the MC matrix (Fig. 1a–c). Conversely, aggregation occurs at 3.0% Cur concentration, resulting in irregularities and surface roughness (Fig. 1d). This can be attributed to the hydrophobic nature of Cur, which makes it difficult to achieve homogeneous dispersion in hydrophilic environments, particularly at higher concentrations.

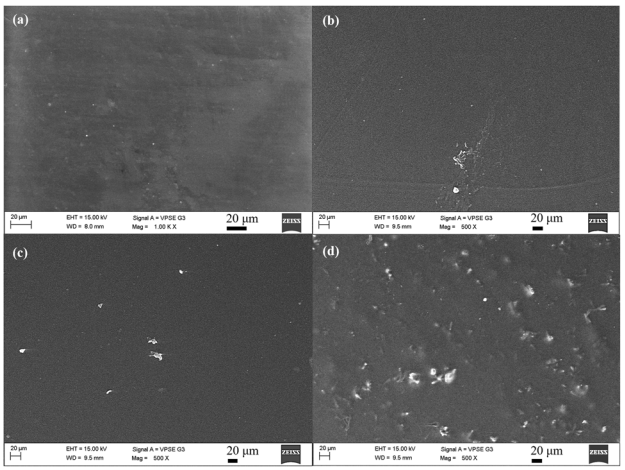


Fig. 1 SEM images of (a) neat MC, (b) MC/0.5% Cur, (c) MC/1.0% Cur, and (d) MC/3.0% Cur films.

### 3.3 Mechanical properties

The thickness, $T_s$, $Y_m$, and %E of MC and MC/Cur films are presented in Table 1. An increase in film thickness was noted with increasing Cur loading, from ~53.59 μm for MC/0.5% Cur to ~57.20 μm for MC/3.0% Cur, corresponding to an ~6.73% increase. A similar increase in thickness has been observed for Cur-loaded biopolymer films, including CMC/1.0% Cur (~14.9%),[26] agar/1.0% Cur (~15.7%), chitosan/1.0% Cur (~1.5%), and carrageenan/1.0% Cur (~11.4%).[27] Ts of the developed films increased with increasing Cur concentration (up to 1.0% Cur loading), followed by a ~27.4% decline for the MC/3.0% film compared to the MC/1.0% Cur film. This decrease is due to the uneven distribution and aggregation of Cur, which can weaken interfacial bonding within the polymer matrix and compromise the structural integrity of the film. This trend aligns with Liu *et al.*,[28] who found that the $T_s$ in cationic starch/deep eutectic solvent/Cur system increased by ~11.3% at 1.0% Cur loading (~17.27 MPa), then decreased by ~16.27% at 5.0% Cur concentration compared to 1.0% Cur incorporation. Similarly, Taghavi Kevij *et al.*,[29] noted that Cur-incorporated whey protein isolate films showed an initial rise in $T_s$ (~38.5%) up to 0.2% Cur incorporation (~2.41 MPa), followed by a decline of ~24.5% at 1.0% Cur compared to 0.2% Cur loading.

Likewise, $Y_m$ increased from ~873.41 MPa for neat MC to ~984.32 MPa for MC/1.0% Cur film before showing a ~26.7% reduction for MC/3.0% Cur film compared to the MC/1.0% Cur film. This suggests that the films became slightly stiffer when incorporated with Cur but then lost rigidity at higher concentrations, likely due to particle aggregation, weakening the overall network structure. A similar trend was observed for CMC/Cur films, where the elastic modulus of neat CMC (~1440 MPa) increased to ~1500 MPa with 0.5% Cur incorporation, but further addition of Cur (1.0 wt%) led to a reduction in elastic modulus to ~1300 MPa.[26] The %E showed a significant increase from ~25.61% for neat MC to 37.17% for the MC/3.0% Cur film. A similar observation was reported by Baek and Song,[30] the %*E*

**Table 1** Thickness, mechanical, antioxidant, UV-blocking, and moisture barrier properties of MC and MC/Cur films[a]

| Films | Thickness (μm) | $T_s$ (MPa) | $Y_m$ (MPa) | %$E$ | DPPH scavenging activity (%) | ABTS scavenging activity (%) | UV-A blocking (%) | UV-B blocking (%) | WVP [$\times 10^{-10}$ g ($m^{-1}$ $s^{-1}$ $Pa^{-1}$)] | WCA (°, $t$ = 5 s) |
|---|---|---|---|---|---|---|---|---|---|---|
| MC | 52.93 ± 3.17$^a$ | 46.71 ± 2.19$^b$ | 873.41 ± 87.15$^b$ | 25.61 ± 0.05$^a$ | 32.57 ± 0.85$^a$ | 25.95 ± 0.43$^a$ | 32.50 ± 0.2$^a$ | 38.57 ± 0.15$^a$ | 4.27 ± 0.19$^a$ | 45.1 ± 0.42$^a$ |
| MC/0.5% Cur | 53.59 ± 3.2$^a$ | 51.35 ± 3.78$^c$ | 913.45 ± 58.87$^b$ | 27.74 ± 0.09$^b$ | 63.19 ± 3.38$^b$ | 62.67 ± 1.49$^b$ | 88.27 ± 0.33$^b$ | 80.85 ± 0.34$^b$ | 3.18 ± 0.68$^b$ | 54.45 ± 0.92$^b$ |
| MC/1.0% Cur | 54.16 ± 2.34$^a$ | 60.23 ± 1.17$^d$ | 984.32 ± 43.23$^c$ | 31.45 ± 0.12$^c$ | 67.88 ± 0.66$^c$ | 65.44 ± 0.73$^c$ | 89.67 ± 0.28$^c$ | 81.55 ± 0.08$^c$ | 3.07 ± 0.01$^b$ | 64.0 ± 0.99$^c$ |
| MC/3.0% Cur | 57.20 ± 4.39$^b$ | 43.73 ± 2.97$^a$ | 721.56 ± 54.12$^a$ | 37.17 ± 1.31$^d$ | 84.26 ± 0.28$^d$ | 90.26 ± 0.21$^d$ | 99.52 ± 0.18$^d$ | 99.31 ± 0.09$^d$ | 1.60 ± 0.04$^c$ | 71.25 ± 0.64$^d$ |

[a] Different superscript letters in the columns are significantly different ($p < 0.05$).

increased from 17.21% for proso millet starch (PMS) to 34.08% for PMS/Cur (3.0%), ascribed to enhanced mobility of polymer chains.

### 3.4 Moisture barrier properties

The WCA and WVP results indicate that the Cur incorporation significantly influenced the films' hydrophobicity and water vapour barrier properties (Table 1). The WCA of the neat MC film (~45.1°) increased by ~20.7%, ~41.9% and ~58.0% with the addition of 0.5%, 1.0%, or 3.0% Cur, respectively. This increase in WCA indicates enhanced hydrophobicity due to the nonpolar nature of Cur, which reduces the affinity for water molecules on the film's surface.[14] These results are consistent with previous studies on CMC/Cur films, where the WCA of neat CMC (~43.2°) increased to ~47.3° and ~49.1° with the incorporation of 0.5 wt% and 1.0 wt% Cur, respectively.[26]

Similarly, the WVP of the films decreased with increasing Cur content. The neat MC film exhibited a WVP of ~4.27 × $10^{-10}$ g ($m^{-1}$ $s^{-1}$ $Pa^{-1}$), which decreased by ~25.5%, ~28.1%, and ~62.5% for the 0.5%, 1.0%, or 3.0% Cur incorporated MC films, respectively. These results are consistent with the reports of Roy *et al.*,[27] where a decrease in WVP was observed when Cur was incorporated into agar, chitosan, and carrageenan. Another study by Musso *et al.*,[13] demonstrated an ~84.6% reduction in WVP for gelatin/0.4% Cur (0.02% w/v) film, further supporting Cur's role as an effective filler in enhancing the moisture barrier of biopolymer films.

### 3.5 Antioxidant and UV blocking properties

The antioxidant activity of the films enhanced significantly upon incorporation of Cur into the MC matrix (Table 1). The DPPH scavenging activity of the neat MC film was ~32.57%, which increased to ~63.19%, ~67.88%, and ~84.26% with the addition of 0.5%, 1.0%, or 3.0% Cur, respectively. Similarly, the ABTS scavenging activity showed a marked improvement from ~25.95% (neat MC) to ~62.67%, ~65.44%, and ~90.26% for the 0.5%, 1.0%, or 3.0% Cur incorporated MC films, respectively. The enhanced antioxidant performance is attributable to Cur's intrinsic ability to neutralise free radicals by donating hydrogen atoms or electrons. This effect is evident in previous findings, wherein the DPPH and ABTS scavenging activities increased to ~86% and ~92% for chitosan (CS)/Cur (5.0%) films, and ~58% and ~29% for pectin/CS/Cur (3.0%) films, respectively.[28,31] The dose-dependent increase in antioxidant activity suggests that higher concentrations of Cur provide more active sites for radical scavenging, thereby improving the overall antioxidant capacity of the biopolymer films.

The UV-blocking properties of MC and MC/Cur films were evaluated in the UV-A (315–400 nm) and UV-B (280–315 nm) regions. The neat MC exhibited relatively low UV-blocking values (~32.50% for UV-A and ~38.57% for UV-B). In contrast, Cur-incorporated films exhibited a stronger UV-blocking effect (Table 1). The MC/3.0% Cur film showed the highest UV blocking, achieving ~99.52% for UV-A and ~99.31% for UV-B. This enhanced UV blocking is attributed to the conjugated π-

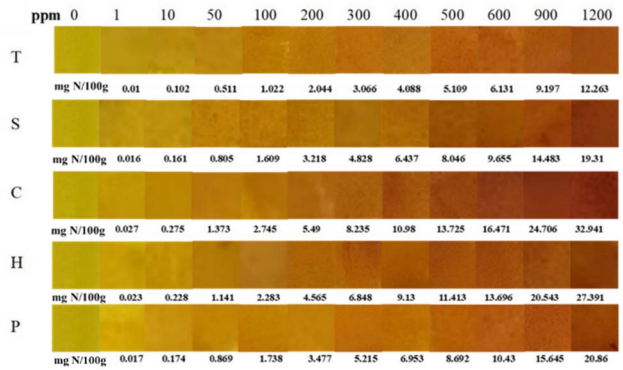


Fig. 2 Response of MC/3.0% Cur intelligent film to varying concentrations (0–1200 ppm) of biogenic amines (T: tyramine, S: apermine, C: cadaverine, H: histamine, P: putrescine).

electrons and phenolic groups in Cur, which effectively absorb UV radiation.[32]

### 3.6 Intelligent film sensitivity against biogenic amines

The MC/3.0% Cur film exhibited a distinct colour change from bright yellow to reddish-brown for cadaverine, spermine, histamine, tyramine, and putrescine (Fig. 2). This pH-induced colour change can be attributed to keto-enol transformation in Cur resulting from elevated biogenic amine levels.[11] The sensitivity of the different biogenic amines to the intelligent film varied significantly, depending on their basicity and volatility.

The MC/3.0% Cur film showed a colour difference $\Delta E \approx 55$ at ~20 mg N/100 g TVB-N for cadaverine, histamine, and putrescine, which corresponds to the regulatory spoilage threshold for chicken meat. This response was substantially higher than that reported for gelatin/methacryloyl films ($\Delta E \approx 20$),[33] carrageenan/CMC/composite anthocyanins film ($\Delta E \approx 45.5$),[34] and chitosan/butterfly pea extract films ($\Delta E \approx 19$).[35] The superior sensitivity of the MC/3.0% Cur film can be attributed to the non-ionic nature of MC[15] with minimal intrinsic buffering capacity. In contrast, gelatin,[36] chitosan,[37] and CMC[15] contain ionisable functional groups (*e.g.*, $NH_2$ and COOH), which can partially buffer pH changes induced by volatile amines.

### 3.7 ML model training and evaluation

The ANN was selected for classification (Table S1) and regression (Table S2) model development as it outperformed linear regression, SVR, logistic regression, SVC, and decision trees models used for testing. The ANN-based regression model exhibited strong predictive performance (Fig. 3, Tables S2 and S3), evidenced by an $R^2$ of 0.928 and a 10-fold cross-validated $R^2$ of 0.940 ± 0.016. The model's accuracy is further supported by a low RMSE of 1.99 mg N/100 g, indicating precise predictions. Similarly, the ANN model (Tables S1 and S3) performed exceptionally well in the classification task, achieving an overall model accuracy of ~96.5% and a 10-fold cross-validated accuracy of 96.3% ± 1.1%. Furthermore, the confusion matrix (Fig. 4a) and ROC-AUC (Fig. 4b) confirmed the model's effectiveness in classifying data into fresh, semi-fresh, or spoiled categories. For the fresh category, the model achieved a precision of 0.991, a recall of 0.953, and an F1 score of 0.972. In the semi-fresh category, the precision was 0.925, the recall was 0.971, and the F1 score was 0.947. The spoiled category's precision was 0.980, the recall was 0.968, and the F1 score was 0.974. Although the ANN model achieved a high overall accuracy (96.5%), misclassifications occurred near freshness boundaries (between fresh: semi-fresh and semi-fresh: spoiled), where the colour transitions of the MC/3.0% Cur film partially overlap. This indicates that classification uncertainty is highest near the regulatory cut-off value, while predictions for clearly fresh or spoiled states remain highly reliable.

The classification accuracy of the MC/3.0% Cur system (96.5%) was comparable to a convolutional neural network-based gelatin/methacryloyl platform (96.2%).[33] This indicates that the MC/3.0% Cur intelligent film achieved high sensing reliability without requiring complex ML architectures.

### 3.8 Application of ML model for shelf-life evaluation of chicken meat

The developed MC/3.0% Cur intelligent film and the integrated ML model were applied to monitor the freshness of chicken meat stored at 4 ± 2 °C. Biogenic amines produced during microbial spoilage induced a visible, quantifiable colour change

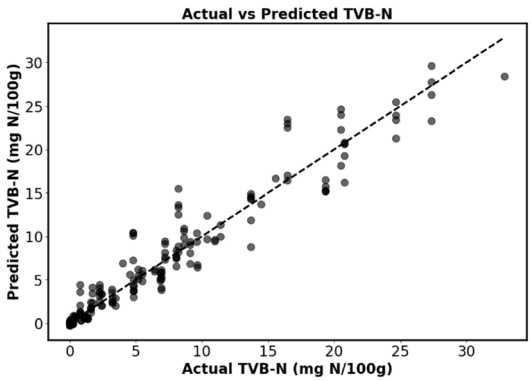


Fig. 3 Actual and predicted TVB-N content (mg N/100 g) from biogenic amines by the regression ANN model.

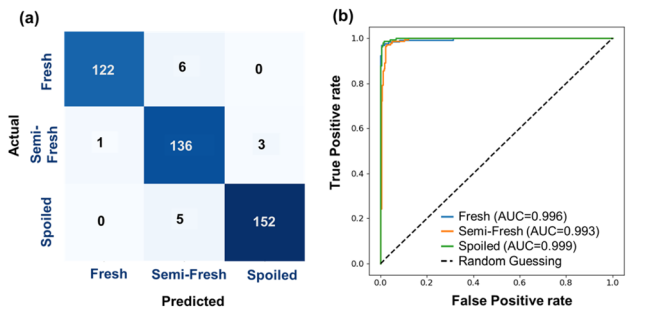


Fig. 4 (a) Confusion matrix, and (b) ROC-AUC of the classification ANN model.

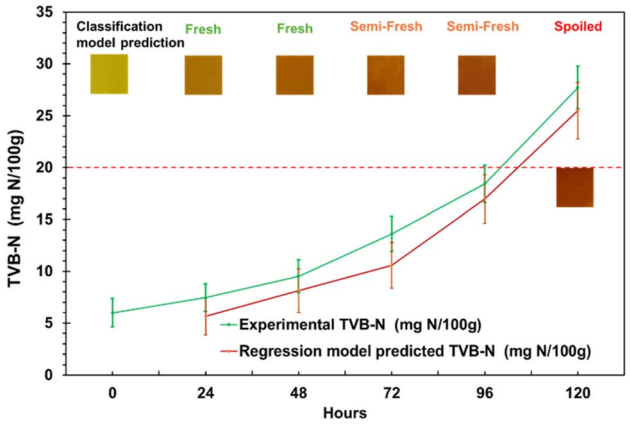


Fig. 5 Classification model prediction (fresh, semi-fresh, or spoiled chicken meat) and regression model predicted *vs.* experimental TVB-N in chicken meat at 4 ± 2 °C.

in the intelligent film. The acceptable limits for pH and TVB-N in chicken meat are ~6.3 and ~20 mg N/100 g, respectively.[6] The pH exhibited a slight decrease from ~5.99 to ~5.65 during 24–48 h, which is characteristic of the post-mortem rigour mortis phase, where glycogen is converted to lactic acid.[38] Following this, the pH gradually increased to ~6.26 after 120 hours, signalling the progression of microbial spoilage. TVB-N levels of the chicken meat gradually increased from ~8.45 mg N/100 g (fresh) to ~14.61 mg N/100 g, (semi-fresh) and finally to ~27.73 mg N/100 g (spoiled) over 120 hours (Fig. 5). The intelligent film displayed a visible colour change from yellow (fresh) to orange (semi-fresh) and finally reddish-brown (spoiled), consistent with the increasing TVB-N and pH.

A high degree of agreement was observed between the ML predicted and experimentally determined TVB-N values for chicken meat samples. The regression ANN model demonstrated strong predictive performance, with an $R^2$ of 0.901. Similarly, the classification ANN model effectively differentiated samples into fresh, semi-fresh, or spoiled, highlighting its reliability in quality assessment. The web-based application successfully integrated the model for real-time analysis, enabling rapid, reliable on-site classification of chicken meat freshness (Fig. 6).

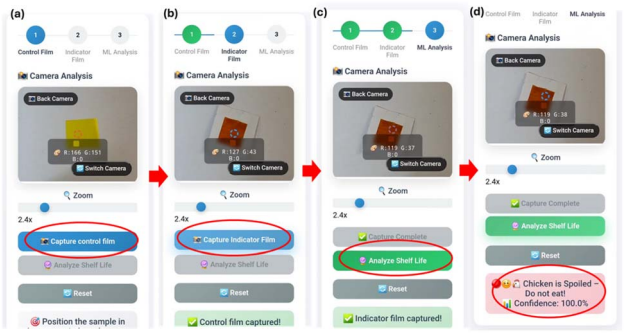


Fig. 6 Workflow of chicken meat freshness monitoring *via* the web-based application: (a) unexposed MC/3.0% Cur intelligent film, (b) chicken meat exposed MC/3.0% Cur intelligent film, (c) shelf-life evaluation through ML model, and (d) ML predicted output.

Although the model training was conducted under controlled lighting conditions, an unexposed, intelligent, film-based colour-correction strategy was incorporated to minimise variations in images acquired across different devices and lighting conditions. This approach partially compensates for variations in illumination and camera colour balance. Also, if the captured image of the chicken meat unexposed intelligent film deviates by more than ±15% from the predefined reference values, the web-based application prompts the user to recapture the photo. However, the implementation of the developed application is limited to lighting/camera conditions similar to those used during model training. Future work can focus on improving robustness by implementing a multi-point colour normalisation method and expanding the training dataset to include images captured with different smartphone devices and under diverse lighting conditions.

## 4 Conclusions

This work demonstrates a food-grade, biodegradable intelligent packaging system that integrates MC/3.0% Cur film with ML for real-time monitoring of chicken meat freshness. This film showed an improved moisture barrier [WCA ~71.2°; WVP ~1.6 × $10^{-10}$ g ($m^{-1}$ $s^{-1}$ $Pa^{-1}$)], antioxidant (DPPH scavenging ~84%; ABTS scavenging ~90%), and UV-blocking properties (>99%). The MC/3.0% Cur intelligent film exhibited distinct pH-responsive colour changes upon exposure to biogenic amines, which were quantitatively captured using a smartphone and translated into colour features for ML analysis. The ANN-based regression model achieved high predictive performance ($R^2$ = 0.928; RMSE = 1.99 mg N/100 g), while the ANN classification model achieved 96.5% accuracy in identifying freshness states. Validation using chicken meat stored at 4 ± 2 °C confirmed a strong correlation between predicted and experimental TVB-N values. While the current model was calibrated for chicken meat spoilage, the underlying TVB-N induced pH sensing mechanism can be applied to other meat types by adjusting spoilage thresholds to meet specific regulatory standards.

## Author contributions

Suresh Chandra Varsha: investigation, methodology, formal analysis, writing – original draft. Ashique Thazheparamban: investigation, methodology, formal analysis, software, writing – original draft. Arunkumar Panneerselvam: conceptualisation, resources, supervision, project administration, writing – review & editing, funding acquisition.

## Conflicts of interest

There are no conflicts of interest to declare.

## Data availability

The data supporting this article are included in the supplementary information (SI). The Python code for ML model training and training data can be found at https://doi.org/

10.5281/zenodo.18642575. Supplementary information: correlation matrix of extracted features, ATR-FTIR spectra, and performance metrics for classification and regression models. See DOI: https://doi.org/10.1039/d5fb00583c.

## Acknowledgements

AP thanks the Director, CSIR-Central Food Technological Research Institute (CFTRI), Mysuru, for the research support through MLP-0305 WP1. SCV would like to thank the Council of Scientific & Industrial Research (CSIR), Ministry of Science & Technology, Government of India, for the CSIR-SRF fellowship. AT would like to thank the University Grants Commission (UGC) for the UGC-SRF fellowship. SCV and AT thank the Director, CSIR-CFTRI, for the opportunity. The authors acknowledge Dr Seema Kumari, Scientist, CSIR-CFTRI, for useful discussions. Vignan Bhavan at the University of Mysore, Mysuru, is acknowledged for SEM analysis. The CSIR-National Institute for Interdisciplinary Science and Technology, Thiruvananthapuram, is acknowledged for WCA analysis.

## References

1 M. T. El-Saadony, A. M. Saad, T. Yang, H. M. Salem, S. A. Korma, A. E. Ahmed, W. F. A. Mosa, T. A. Abd El-Mageed, S. Selim, S. K. Al Jaouni, R. A. Zaghloul, M. E. Abd El-Hack, K. A. El-Tarabily and S. A. Ibrahim, Avian campylobacteriosis, prevalence, sources, hazards, antibiotic resistance, poultry meat contamination, and control measures: a comprehensive review, *Poult. Sci.*, 2023, **102**, 102786.

2 H. T. Thames and A. Theradiyil Sukumaran, A Review of Salmonella and Campylobacter in Broiler Meat: Emerging Challenges and Food Safety Measures, *Foods*, 2020, **9**, 776.

3 Z. Tan, Z. Huang, Y. Lv, Y. Li and D. Chen, A gas Fourier transform infrared spectroscopy methodology for the rapid and accurate discrimination of chicken spoilage through volatiles analysis, *Flavour Fragrance J.*, 2019, **34**, 271–279.

4 L. Esposito, D. Mastrocola and M. Martuscelli, Approaching to biogenic amines as quality markers in packaged chicken meat, *Front. Nutr.*, 2022, **9**, 966790.

5 M. Silva and I. Moln, Quantitation by HPLC of Amines as Dansyl Derivatives, Quantitation of Amino Acids and Amines by Chromatography, *J. Chromatogr. Libr.*, 2005, **70**, 445–470.

6 E. Yildiz, G. Sumnu and L. N. Kahyaoglu, Monitoring freshness of chicken breast by using natural halochromic curcumin loaded chitosan/PEO nanofibers as an intelligent package, *Int. J. Biol. Macromol.*, 2021, **170**, 437–446.

7 M. Ahmed, I. Bose, Nousheen and S. Roy, Development of Intelligent Indicators Based on Cellulose and Prunus domestica Extracted Anthocyanins for Monitoring the Freshness of Packaged Chicken, *Int. J. Biomater.*, 2024, **2024**, 7949258.

8 S. R. Kanatt, Development of active/intelligent food packaging film containing *Amaranthus* leaf extract for shelf life extension of chicken/fish during chilled storage, *Food Packag. Shelf Life*, 2020, **24**, 100506.

9 Z. Aghaei, B. Emadzadeh, B. Ghorani and R. Kadkhodaee, Cellulose Acetate Nanofibres Containing Alizarin as a Halochromic Sensor for the Qualitative Assessment of Rainbow Trout Fish Spoilage, *Food Bioprocess Technol.*, 2018, **11**, 1087–1095.

10 S. Roy, P. Ezati, D. Biswas and J.-W. Rhim, Shikonin Functionalized Packaging Film for Monitoring the Freshness of Shrimp, *Materials*, 2022, **15**, 6615.

11 K. H. Erna, W. X. L. Felicia, K. Rovina, J. M. Vonnie and N. Huda, Development of curcumin/rice starch films for sensitive detection of hypoxanthine in chicken and fish meat, *Carbohydr. Polym. Technol. Appl.*, 2022, **3**, 100189.

12 J. Liu, H. Wang, P. Wang, M. Guo, S. Jiang, X. Li and S. Jiang, Films based on κ-carrageenan incorporated with curcumin for freshness monitoring, *Food Hydrocoll.*, 2018, **83**, 134–142.

13 Y. S. Musso, P. R. Salgado and A. N. Mauri, Smart edible films based on gelatin and curcumin, *Food Hydrocoll.*, 2017, **66**, 8–15.

14 M. Cvek, U. C. Paul, J. Zia, G. Mancini, V. Sedlarik and A. Athanassiou, Biodegradable Films of PLA/PPC and Curcumin as Packaging Materials and Smart Indicators of Food Spoilage, *ACS Appl. Mater. Interfaces*, 2022, **14**, 14654–14667.

15 M. He, Y. Lin, Y. Huang, Y. Fang and X. Xiong, Research Progress of the Preparation of Cellulose Ethers and Their Applications: A Short Review, *Molecules*, 2025, **30**, 1610.

16 X. Li, D. Liu, Y. Pu and Y. Zhong, Recent Advance of Intelligent Packaging Aided by Artificial Intelligence for Monitoring Food Freshness, *Foods*, 2023, **12**, 2976.

17 V. Doğan, M. Evliya, L. Nesrin Kahyaoglu and V. Kılıç, On-site colorimetric food spoilage monitoring with smartphone embedded machine learning, *Talanta*, 2024, **266**, 125021.

18 F. Mazur, Z. Han, A. D. Tjandra and R. Chandrawati, Digitalization of Colorimetric Sensor Technologies for Food Safety, *Adv. Mater.*, 2024, **36**, 2404274.

19 ASTM International, *E96/E96M-Standard Test Methods for Gravimetric Determination of Water Vapor Transmission Rate of Materials, ASTM International, 100 Barr Harbor Drive, PO Box C700, West Conshohocken, PA 19428-2959*, United States, DOI: 10.1520/E0096_E0096M-24.

20 ASTM International, *ASTM-D882 Standard Test Method for Tensile Properties of Thin Plastic Sheeting, ASTM International, 100 Barr Harbor Drive, PO Box C700, West Conshohocken, PA 19428-2959*, United States, DOI: 10.1520/D0882-18.

21 S. Chandra Varsha, B. K. Bettadaiah and A. Panneerselvam, Multifunctional Tetrahydrocurcumin Reinforced Methylcellulose Films for Shelf Life Evaluation of Chicken Meat, *Food Control*, 2026, **182**, 111798.

22 D. Singh and B. Singh, Investigating the impact of data normalization on classification performance, *Appl. Soft Comput.*, 2020, **97**, 105524.

23 J. Cai, Q. Chen, X. Wan and J. Zhao, Determination of total volatile basic nitrogen (TVB-N) content and Warner-

Bratzler shear force (WBSF) in pork using Fourier transform near infrared (FT-NIR) spectroscopy, *Food Chem.*, 2011, **126**, 1354–1360.

24 C. L. de Dicastillo, F. Bustos, A. Guarda and M. J. Galotto, Cross-linked methyl cellulose films with murta fruit extract for antioxidant and antimicrobial active food packaging, *Food Hydrocoll.*, 2016, **60**, 335–344.

25 L. Zhang, L. Xu, J.-K. Ma, Y.-Y. Ye, Y. Chen and J.-Y. Qian, Introduction of Curdlan Optimizes the Comprehensive Properties of Methyl Cellulose Films, *Foods*, 2023, **12**, 547.

26 S. Roy and J. W. Rhim, Carboxymethyl cellulose-based antioxidant and antimicrobial active packaging film incorporated with curcumin and zinc oxide, *Int. J. Biol. Macromol.*, 2020, **148**, 666–676.

27 S. Roy and J.-W. Rhim, Preparation of carbohydrate-based functional composite films incorporated with curcumin, *Food Hydrocoll.*, 2020, **98**, 105302.

28 Y. Liu, M. Liu, L. Zhang, W. Cao, H. Wang, G. Chen and S. Wang, Preparation and properties of biodegradable films made of cationic potato-peel starch and loaded with curcumin, *Food Hydrocoll.*, 2022, **130**, 107690.

29 H. Taghavi Kevij, M. Salami, M. Mohammadian and M. Khodadadi, Fabrication and investigation of physicochemical, food simulant release, and antioxidant properties of whey protein isolate-based films activated by loading with curcumin through the pH-driven method, *Food Hydrocoll.*, 2020, **108**, 106026.

30 S. Baek and K. B. Song, Characterization of Active Biodegradable Films Based on Proso Millet Starch and Curcumin, *Starch*, 2019, **71**, 1800174.

31 Q. Xie, X. Zheng, L. Li, L. Ma, Q. Zhao, S. Chang and L. You, Effect of curcumin addition on the properties of biodegradable pectin/chitosan films, *Molecules*, 2021, **26**, 2152.

32 A. Botalo, T. Inprasit, S. Ummartyotin, K. Chainok, S. Vatthanakul and P. Pisitsak, Smart and UV-Resistant Edible Coating and Films Based on Alginate, Whey Protein, and Curcumin, *Polymers*, 2024, **16**, 447.

33 W. Gong, H.-B. Yao, T. Chen, Y. Xu, Y. Fang, H.-Y. Zhang, B.-W. Li and J.-N. Hu, Smartphone platform based on gelatin methacryloyl(GelMA)combined with deep learning models for real-time monitoring of food freshness, *Talanta*, 2023, **253**, 124057.

34 Y. Cao, Q. Gou, Z. Song, L. Zhang, Q. Yu, X. Zhu and S. Li, Smart carrageenan/carboxymethyl cellulose films combined with zein/gellan gum microcapsules encapsulated by composite anthocyanins for chilled beef freshness monitoring, *Food Hydrocoll.*, 2024, **153**, 110059.

35 J. Yan, R. Cui, Y. Qin, L. Li and M. Yuan, A pH indicator film based on chitosan and butterfly pudding extract for monitoring fish freshness, *Int. J. Biol. Macromol.*, 2021, **177**, 328–336.

36 J. Baty and T. Barrett, Gelatin Size as a PH and Moisture Content Buffer in Paper, *J. Am. Inst. Conserv.*, 2007, **46**, 105–121.

37 C. Moreira, H. Oliveira, L. R. Pires, S. Simões, M. A. Barbosa and A. P. Pêgo, Improving chitosan-mediated gene transfer by the introduction of intracellular buffering moieties into the chitosan backbone, *Acta Biomater.*, 2009, **5**, 2995–3006.

38 N. A. Mir, A. Rafiq, F. Kumar, V. Singh and V. Shukla, Determinants of broiler chicken meat quality and factors affecting them: a review, *J. Food Sci. Technol.*, 2017, **54**, 2997–3009.